

# MSMD-Net: Deep Stereo Matching with Multi-scale and Multi-dimension Cost Volume

Zhelun Shen  
Northwestern Polytechnical  
University  
Peking University  
shenzhelun@pku.edu.cn

Yuchao Dai\*  
Northwestern Polytechnical  
University  
Corresponding Author  
daiyuchao@nwpu.edu.cn

Zhibo Rao  
Northwestern Polytechnical  
University  
raoxi36@foxmail.com

## ABSTRACT

Deep end-to-end learning based stereo matching methods have achieved great success as witnessed by the leaderboards across different benchmarking datasets (KITTI, Middlebury, ETH3D, etc), where the cost volume representation is an indispensable step to the success. However, most existing work only employs a *single* cost volume, which cannot fully exploit the multi-scale cues in stereo matching and provide guidance for disparity refinement. What's more, the single cost volume representation also limits the disparity range and the resolution of the disparity estimation. In this paper, we propose MSMD-Net (Multi-Scale and Multi-Dimension) to construct *multi-scale* and *multi-dimension* cost volume. At the multi-scale level, we generate four 4D combination volumes at different scales and integrate them in 3D cost aggregation to predict an initial disparity estimation. At the multi-dimension level, we construct a 3D warped correlation volume and use it to refine the initial disparity map with residual learning. These two dimensional cost volumes are complementary to each other and can boost the performance of disparity estimation. Additionally, we propose a switch training strategy to further improve the accuracy of disparity estimation, where we switch two kinds of different activation functions to alleviate the overfitting issue in the pre-training process. Our proposed method was evaluated on several benchmark datasets and ranked first on KITTI 2012 leaderboard and second on KITTI 2015 leaderboard as of June 23. The code of MSMD-Net is available at <https://github.com/gallenszl/MSMD-Net>.

## KEYWORDS

Stereo matching, Cost volume, Activation functions, Multi-scale

## 1 INTRODUCTION

Stereo matching aims at estimating the disparity map between a rectified image pair, which is of great importance to various applications such as autonomous driving [3] and robotics navigation [1]. Recently, the unprecedented advancement of deep learning in high level vision tasks has been extended to geometric problems such as stereo matching. Currently, deep end-to-end learning-based approaches have achieved state-of-the-art performance on most of the standard stereo matching benchmarks, *i.e.*, KITTI, Middlebury and ETH3D.

In the network architecture design, the deep learning-based approaches generally follow the traditional stereo matching pipeline, *i.e.*, feature extraction, cost volume construction, cost aggregation and disparity optimization. The cost volume construction module produces initial similarity measures for left image patches and

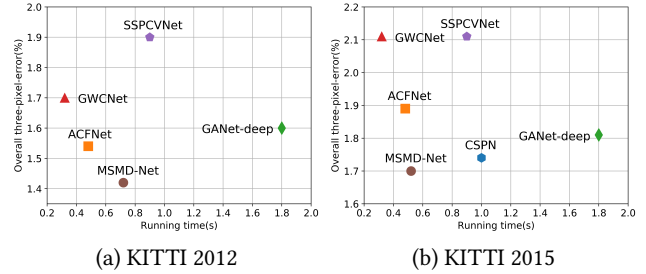
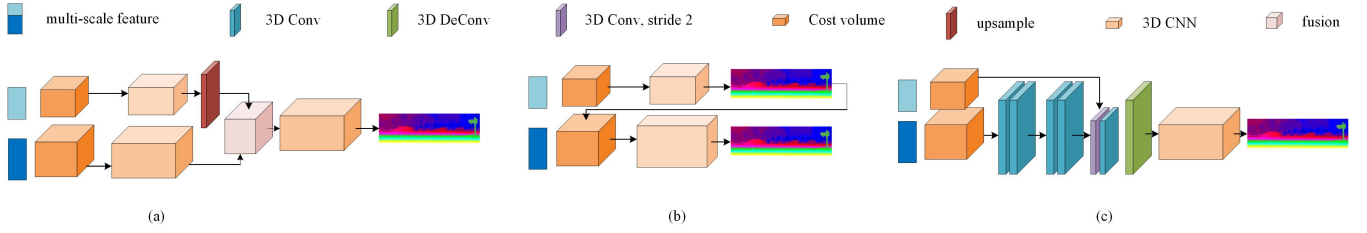


Figure 1: Disparity estimation accuracy and run-time comparison with state-of-the-art methods on KITTI.

possible corresponding right patches, which has been proved as a crucial step in achieving accurate disparity estimation. Existing work have exploited different forms of cost volume [10, 16, 19] to effectively measure the similarity between patches. Dispnet [19] utilizes the correlation volume to measure feature similarities between the left features and its shifted right features. GCNet [16] concatenates the left features and shifted right features directly to generate a 4D concatenation feature volume and employs 3D convolutions to regularize it. GWCNet [10] divides the unary feature into groups and calculates correlation maps in each group to preserve the measurement of feature similarities, which can be viewed as an intermedia operation between computing the correlation of features and concatenating features directly. Multi-scale information has been exploiting in [2, 17, 22] to construct cost volume for better encoding global and local information, which helps the network to learn the context relationship between an object (for example, a house) and its sub-regions (windows, doors, etc.). However, most of these work only generate a *single cost volume* at a fixed scale for cost aggregation, which can't effectively utilize the multi-scale information and provide guidance to disparity refinement.

In this paper, we propose MSMD-Net to construct multi-scale and multi-dimension cost volume to tackle above problems. At the multi-scale level, we use the corresponding extracted feature to generate a 4D combination volume at each scale. Specifically, the combination volume is composed of concatenation volume and group-wise correlation volume, and then the multi-scale combination volume will be integrated together to predict an initial disparity in the cost aggregation step. Even though idea of employing multi-scale cost volume has also been investigated in [4, 9, 28, 30], our work differs from theirs in the following two main aspects: 1) We build multi-scale cost volume explicitly with both feature concatenation and group-wise correlation, which is more discriminative



**Figure 2: Comparison between different methods of employing multi-scale cost volume. (a) SSPCV [28], (b) cascade volume [4, 9, 30] and (c) our proposed cost volume integration module. Note that, to simplify the illustration, we assume that all methods only use two different scale cost volumes. Extension the number of cost volume is straightforward. We also omit the skip connection for better visual contrast.**

than single feature concatenation; 2) [4, 9, 30] propose cascade volume to respectively use multi-scale cost volume and iteratively narrow the disparity range and refine depth maps in a coarse-to-fine manner. SSPCV [28] integrates the multi-scale cost volume by gradually upsampling the lowest scale to the highest. However, these two methods both have several drawbacks. The cascade volume loses much information during the process of reducing the disparity range and SSPCV needs a large training parameter to constantly employ 3D hourglass modules to regularize the upsampled cost volume. Instead, we design a cost volume integration module to fuse multi-scale cost volume in an encoder-decoder process, which preserves the whole disparity range and decreases the number of 3D hourglass modules at the same time. The visual comparison can be seen in Figure 2.

At the multi-dimension level, we additionally introduce 3D warped correlation volume for disparity refinement. Specifically, the warped correlation volume is calculated by the left feature and reconstructed left feature (warped right feature) following the construction principle proposed in DispNet [19]. It measures the similarities between left feature and reconstructed left feature (warped right feature) at each disparity level and define a possible and fine-grained disparity confidence range between initial disparity map and ground-truth. And the mission of the refinement network is to pick out the most similar disparity level in each pixel with the support of context information such as the left feature, reconstructed error, and the initial disparity map. The insight of disparity refinement has also been investigated in deep stereo matching methods such as [6, 17, 23, 27]. For these previous work, they mainly depend on the network to automatically learn a map between input information and residue without employing the geometry of stereo vision. Comparing with directly using context information to regress the residue, the warped correlation volume makes the input of refinement network more interpretable. Note that the warped correlation volume is 3D cost volume and the multi-scale combination volume is 4D cost volume. These two different dimensional cost volumes are complementary to each other and play different roles in our network, so we can say that we calculate cost volume at multiple scales and dimensions.

Moreover, we find that overfitting issues may appear when we extend the pre-training process on the SceneFlow datasets. It shows up as a performance improvement on the SceneFlow datasets but no significant change on the KITTI datasets. In order to alleviate

this issue, we propose a switch training strategy. Specifically, we first use the Relu [11, 15, 21] function to pretrain our model and then switch the activation function to Mish [20] to prolong the pre-training process on the SceneFlow dataset. Experiments have shown the effectiveness of our switching training strategy compared with using a single activation function. We use it to further boost the performance and the comparison between our method with some state-of-the-art methods [5, 10, 28, 33, 34] can be seen in Figure 1.

Our main contributions are summarized as:

- To exploit the multi-scale information, we calculate multi-scale 4D combination cost volumes and develop a cost volume integration module to fuse them for cost aggregation.
- We introduce a 3D warped correlation volume as an input of refinement network to make the refinement step more interpretable.
- We propose a switch training strategy to alleviate the overfitting issues during the extension of pre-training iterations on the SceneFlow datasets.
- We achieved state-of-the-art accuracy on the KITTI dataset and ranked first on KITTI 2012 leaderboard and second on KITTI 2015 leaderboard as of June 23.

## 2 RELATED WORK

**CNN for matching cost computation:** Estimating depth from a rectified image pair is a classical problem which has been studied for decades. D. Scharstein and R. Szeliski [25] conclude that a typical stereo matching algorithm can be divided into four steps: matching cost computation, cost aggregation, optimization, and disparity refinement. Early learning-based work [18, 32] try to replace one or more stereo matching steps with a convolutional neural network. Zbontar and LeCun [32] introduce the first learning-based method, which computes matching cost with a deep Siamese network but it still uses traditional cost aggregation, SGM to predict disparity map. Luo [18] et al further introduce a product layer to compute the inner product between two representations of a Siamese architecture and treat the problem as multi-class classification which significantly reduces the computational complexity.

**End-to-end deep stereo matching without refinement:** DispNet [19] is a real breakthrough which first proposes to construct a correlation cost volume and directly regresses the disparity map

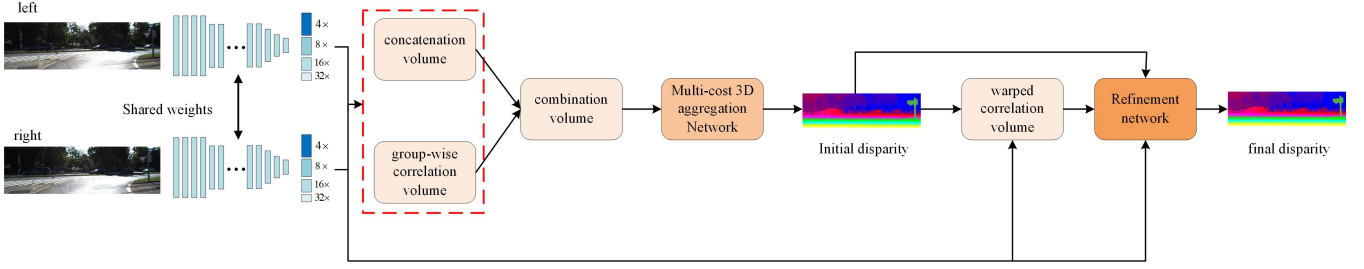


Figure 3: Network architecture of our proposed framework, which consists of 4 consecutive modules: feature extraction, 4D multi-scale combination volume for cost aggregation, 3D warped correlation volume for disparity refinement, and disparity prediction.

in an end-to-end way. Other than DispNet, GCNet [16] proposes to construct concatenation volume and regularize it with 3D convolution layers. Based on GCNet, PSMNet [2] introduces a Spatial Pyramid Pooling Module and stacked hourglass 3D CNN for better feature extraction and cost aggregation. GWCNet [10] introduces group-wise correlation to provide better similarity measures than previous work and it can cooperate with the concatenation volume to further improve the performance. Following these work, ACFNet [34] solves the uncertain distribution of cost volume by directly using unimodal ground truth distributions to supervise cost volume.

**End-to-end deep stereo matching with refinement:** Recently, many researchers [6, 17, 23, 26, 27] attempt to integrate the disparity refinement step into an end-to-end learning model. Pang et al [23] introduce a two-stage network called CRL in which the first stage extends DispNet [19] to get an initial disparity map with more details and the second stage refines the initial disparity map in a residual manner. Different from CRL, Liang et al [17] propose to calculate reconstruction error in feature space rather than colour space and share features between disparity estimation network and refinement network. Sun et al [26] propose a context network, which is based on dilated convolutions to refine flow. Following PWC-Net, [6, 27] construct a similar refinement network using left image features and the initial disparity map. Different from these work, here we introduce the warped correlation cost volume to guide the disparity refinement. Specifically, we use left image features and warped right image features to construct the warped correlation cost volume, hoping it can learn the difference between initial disparity map and ground truth with the help of other information like reconstruction error and left image features.

**End-to-end deep stereo matching using multi-scale information:** Multi-scale information has been widely employed in stereo estimation. PSM-Net [2] introduces SPP module to generate feature maps at different levels. Liang et al [17] proposes a shallow encoder-decoder architecture to extract multi-scale features of the original picture. However, most existing work only use multi-scale features to construct a single volume at a fixed resolution other than considering them separately. Some work [4, 9, 28, 30] also discover this issue and give some resolutions to employ multi-scale cost volume. [4, 9, 30] proposes to construct cascade multi-scale cost volume and progressively regress a high-quality disparity map. Specifically, they use the coarsest cost volume to generate an initial

disparity map and then narrow the disparity range of each stage by the prediction from the previous stage. With gradually higher cost volume resolution and adaptive adjustment of disparity intervals, the output is recovered in a coarser to fine manner. Comparing with estimating disparity map at each scale respectively, our work introduces an encoder-decoder process to directly integrate different scale cost volumes to capture more robust global and local feature representation for the regularization of cost volume. Our method is a little similar to SSPCV [28] but using a totally different cost integration way to get faster speed and better accuracy.

### 3 OUR APPROACH

In this section, we first describe the overall network architecture of our MSMD-Net and then provide details of our proposed *multi-scale* and *multi-dimension* cost volume module. At the multi-scale level, we propose a 4D multi-scale cost volume to effectively exploit the multi-scale cues for accurate disparity estimation. At the multi-dimension level, to further improve the initial disparity estimation, we propose to use an additional 3D warped correlation volume to refine the initial disparity with residual learning.

#### 3.1 Network Architecture

Our network architecture is illustrated in Figure 3, which consists of four parts: feature extraction, 4D multi-scale combination volume for cost aggregation, 3D warped correlation volume for disparity refinement, and disparity prediction.

**Feature extraction:** Following the Resnet-like network proposed in [2, 10], we use three convolution layers of  $3 \times 3$  kernels, four basic residual blocks and a 2 dilated block to get the unary feature map of first scale (1/4 of the original input image size). In order to construct multi-scale cost volume, we further employ three residual blocks with stride 2 to get feature maps at different scales.

**4D Multi-scale combination volume for cost aggregation:** We use the multi-scale feature maps to generate four corresponding scale 4D combination volumes with the method introduced in [10]. These multi-scale cost volumes will be merged during encoder-decoder process in cost volume integration module and then we use three stacked 3D hourglass networks to learn more context information with repeated top-down/bottom-up processing.

**3D warped correlation volume for disparity refinement:** We employ the 3D warped correlation volume to give a guide to disparity refinement. Specifically, the 3D warped correlation volume is

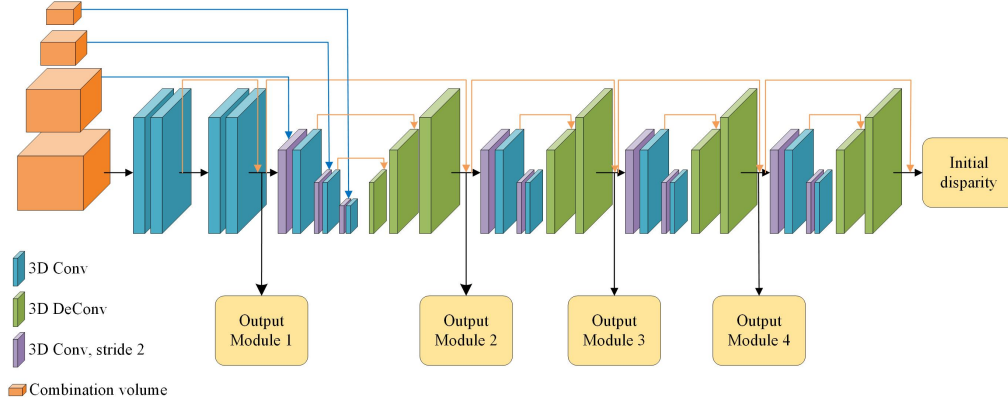


**Figure 4: Detailed structure of our multiple cost 3D aggregation network. Compared with GWCNet [10], it adds an additional cost volume integration module to merge different scale cost volumes. Note that the output module is only be applied during the training process.**

calculated by the left feature and warped right feature and it identifies a confidence range between the initial disparity and ground truth. Then other information is added to drive the network to pick out the most possible disparity level by residual learning.

**Disparity prediction:** In addition to the final disparity map, every submodule in 3D cost aggregation will predict a disparity map by the same output module and soft argmin operation [16]. Thus our network has six outputs during the training phase and the final loss is a weighted sum of these outputs.

### 3.2 4D Multi-scale Combination Volume for Cost Aggregation

Previously, three different kinds of cost volumes have been proposed: 1) correlation volume [17, 19] 2) concatenation volume [2, 16] and 3) group-wise correlation volume [10]. Correlation volume uses dot products to measure feature similarities between a left feature and its shifted right features. It is efficient but loses much information because of the decimation of feature channel. Concatenation volume directly concatenates the left features and shifted right features. It generates a 4D volume without the decimation of feature channel but requires more parameters to train in cost aggregation. Group-wise correlation volume divides unary feature into groups and calculates correlation maps in each group. Compared with concatenation volume, it preserves the measurement of feature similarities but still needs a lot of parameters to train. Moreover, the second and third method have been proved to be complementary to each other.

For every cost volume construction method, improving the representation ability of features can definitely construct a better cost volume and further boost the performance of depth estimation. Recent work [2, 17, 22] have shown that using multi-scale information can improve the network performance. However, most of them only construct a single cost volume which can't fully utilize the multi-scale information.

To effectively exploit the multi-scale cues for disparity estimation, we propose to calculate a 4D multi-scale combination volume

for cost aggregation. Specifically, we employ the extracted multi-scale feature to construct combination volume, which is constituted of concatenation volume and group-wise correlation volume. We denote the extracted multi-scale feature as  $f^i$ , where  $i$  means the  $i^{th}$  scale and  $i = 1$  represents the highest scale (1/4 of the original input image size). The concatenation volume is computed as:

$$V_{concat}^i(d, x, y, f) = f_L^i(x, y) || f_R^i(x - d, y), \quad (1)$$

where  $||$  denotes the vector concatenation operation at the feature dimension and group-wise correlation volume is computed as:

$$V_{gwc}^i(d, x, y, g) = \frac{1}{N_c^i / N_g} \langle f_L^{ig}(x, y), f_R^{ig}(x - d, y), \rangle \quad (2)$$

where  $N_c$  represents the channels of the extracted feature.  $N_g$  is the number of group and  $\langle \cdot, \cdot \rangle$  represents the inner product. We use the concatenation operation to get final multi-scale combination volume

$$V_{combine}^i = V_{concat}^i || V_{gwc}^i. \quad (3)$$

Note that when generating group-wise correlation volume, compared with GWCNet, we add one more convolution layer without activation function and batch normalization to make it own the same data distribution with concatenation volume. It optimizes the combination volume and makes it suitable for all datasets so we don't need to use different cost volumes to fit different datasets like GWCNet. Then the multi-scale combination volume will be employed for cost aggregation.

The stacked hourglass architecture [2, 10, 34] has shown its efficiency in cost aggregation and we extend the stacked hourglass architecture with a cost volume integration module to employ multi-scale 4D combination volumes. As shown in Figure 4, the architecture of our cost volume integration module is similar to the hourglass network for maintaining a uniform structure. Additionally, we extend the original architecture to 1/32 the size of the original image and integrate corresponding scale combination volume into the down-sampled cost volume by concatenation operation at the feature dimension (see blue lines in Figure 4). Specifically, we first employ a 3D convolution layer with stride two to



downsample the first scale combination volume (1/4 of the original input image size) to 1/8 of the original input image size. Then we concatenate the down-sampled cost volume and the second scale combination volume at the feature dimension and use one additional 3D convolution layer to decrease the feature channel to a fixed size. Similar operation is progressively employed until we downsample the cost volume to 1/32 of the original input image size. Finally, 3D transposed convolution is employed to progressively up-sample the volume to 1/4 of the original input image size. The feature dimension is set as 32, 64, 128, 128 from the first scale to the last and the  $1 \times 1 \times 1$  3D convolution in the shortcut connection is still preserved to improve the performance (see yellow lines in Figure 4). Then we use three stacked 3D hourglass networks to further regularize and refine the volume. Finally, an output module is employed to predict the disparity. The output module uses two more 3D convolution layers to get a 1-channel 4D volume, then it upsamples the 1-channel 4D volume to the original image size ( $H \times W \times D$ ) and applies soft argmin operation [16] to generate initial disparity map.

### 3.3 3D Warped Correlation Volume for Disparity Refinement

Disparity refinement is an essential step in typical stereo matching algorithm to identify inaccurate regions for post-processing. Recently, several pieces of work try to integrate disparity refinement into an end-to-end network to improve the performance of stereo matching. Residual learning [13] has been proved to be an effective manner [6, 17, 23, 26] and the reconstruction error [17] is introduced to play the role of left-right consistency check in traditional stereo matching.

Different from these work, we introduce the 3D warped correlation volume to make our network more interpretable and boost the performance. Specifically, we use the left feature and warped right feature to construct the 3D warped correlation volume. The disparity between left feature and warped right feature is usually small so we can search a smaller disparity range to refine the initial disparity map with fine-grained correspondences. The warping operation is implemented differentially by bilinear sampling [14]. The 3D warped correlation volume is computed as:

$$V_{warpedcorr}(d, x, y) = \frac{1}{N_c} \langle f_l(x, y), f_{wr}(x - d, y) \rangle \quad (4)$$

where  $f_l$  and  $f_{wr}$  are upsampled from the first scale feature to the original image size. Note that the warped correlation volume measures the similarities between left feature and shifted reconstructed left feature (warped right feature) at each disparity level. We hope the network can pick out the most similar disparity level with the help of context information. That is the network calculates the residual between the initial disparity map and ground truth and such approach is complementary to the residual learning. In addition, the warped correlation volume is a 3D cost volume ( $H \times W \times D$ ), compared with 4D combination volume, such design makes it possible to be regularized at the original image size with an acceptable run-time and GPU memory.

All in all, we use the warped correlation volume, initial disparity map, left feature and reconstructed error as the input of our refinement network. Compared with directly using initial disparity, we

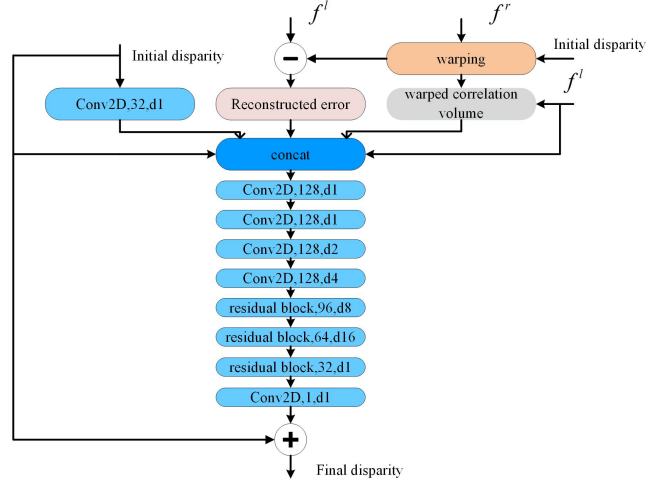


**Figure 5: Detailed structure of our refinement network. The network takes the warped correlation volume, reconstructed error, initial disparity, and the left feature as input and then employs four convolution layers, three basic residual blocks and another one convolution layer (without BN/Relu) to get the residual pixel-wise correction. Note that the dilation rate is defined as  $d$  followed by the value.**

use a convolution layer to generate a 32-channel initial disparity feature map to increase the weight of initial disparity map in the input formation. In addition, the reconstructed error is computed by the left feature and the warped right feature as:

$$E_{reconstruct} = f_l(x, y) - f_{wr}(x, y). \quad (5)$$

The architecture of our refinement network is shown in Figure 5. We use a dilated convolution [31] based network to enlarge the receptive field so that network can better refine low-texture ambiguities and occluded regions. Specifically, it is composed of 5 convolution layers and three basic residual blocks with different dilation constants. The dilation constants are 1,1,2,4,8,16,1 and 1 from top to bottom.

Compared with previous work, the input of our network is more interpretable. The warped correlation volume identifies a fine-grained disparity range between initial disparity map and ground truth. The reconstructed error shows the incorrect regions which should be improved in the refinement step. The initial disparity map gives a baseline of our disparity estimation and the left feature contains enough context informing for residual learning. Reconstructed error, initial disparity map, and left feature cooperate with each other to support the network to find the most similar disparity level in the warped correlation volume at pixel-wise level.

### 3.4 Loss Function

We employ smooth  $L_1$  loss function to train our network in an end-to-end way. For each submodule in 3D cost aggregation, same output module and soft argmin operation are used to get intermediate disparity map. In total, we get six disparity maps  $d_0, d_1, d_2, d_3, d_4, d_5, d_6$

and the loss function is described as:

$$L = \sum_{i=0}^{i=5} w_i \cdot \text{Smooth}_{L_1}(d_i - \hat{d}) \quad (6)$$

in which

$$\text{Smooth}_{L_1}(x) = \begin{cases} 0.5x^2, & \text{if } |x| < 1 \\ |x| - 0.5, & \text{otherwise} \end{cases} \quad (7)$$

where  $\hat{d}$  represents the ground-truth disparity and  $w_i$  is the weight of the  $i^{th}$  estimation of disparity map.

## 4 EXPERIMENT

In this section, we evaluate our proposed model on two datasets: Scene Flow datasets [19] and KITTI datasets [7, 8] and compare it with several state-of-the-art architectures. We also employ ablation studies to evaluate the influence of the proposed multiple cost 3D aggregation and disparity refinement network. Furthermore, we introduce a novel training strategy with a switch between two different activation functions.

### 4.1 Dataset

**SceneFlow:** This is a large synthetic dataset with 35,454 training and 4,370 test images of size  $960 \times 540$  for optical flow and stereo matching. It is composed of Flyingthings3D, Driving, and Monkaa with dense and accurate ground-truth disparity maps for training. Following the setting of GWCNet, we use the Finalpass of the Scene Flow datasets and only employ loss computation in the pixels which are in our predefined disparity range ( $0 < d < d_{\max}$ )

**KITTI 2015 & KITTI 2012:** These two datasets are both real-world dataset collected from a driving car. KITTI 2015 contains 200 training and another 200 testing image pairs while KITTI 2012 provides 194 training and another 195 testing image pairs. Every training image pair is provided a sparse ground-truth disparity collected using LIDAR. For both datasets, we use 180 training image pairs as a training set and the rest as a validation set.

**Table 1: Ablation study results of our switch training strategy on SceneFlow and KITTI 2015 validation sets.**

Train Strategy	Scene Flow EPE(px)	KITTI 2015 D1_all(%)
Relu(20 epochs)	0.9841	1.50
Mish(20 epochs)	0.9379	1.46
Mish(35 epochs)	0.8528	1.44
Relu(20 epochs)+Mish(15 epochs)	<b>0.8197</b>	<b>1.40</b>

### 4.2 Implementation Details

we use pytorch to implement our network, and the whole network is trained in an end-to-end way with Adam ( $\beta_1 = 0.9, \beta_2 = 0.999$ ). Inspired by HSM-Net [29], we employ asymmetric chromatic augmentation and asymmetric occlusion for data augmentation. Specifically, we apply different chromatic augmentation to the image pairs hoping our network can improve its robust when stereo cameras are under different lighting and exposure conditions. And we randomly replace a rectangle region at target image with the RGB

means of the whole picture so that our network can learn to predict the disparity without correspondences.

Switch training strategy is employed to train our model and it can be divided into three steps. First, we use Relu to train our network from scratch in SceneFlow dataset for 20 epochs. The initial learning rate is 0.001 and is down-scaled by 2 after epoch 12, 16, 18. Second, we use Mish to prolong the pre-training process in SceneFlow dataset for another 15 epochs. Third, we finetune our pre-trained model in KITTI 2015 and KITTI 2012 for another 400 epochs. The learning rate of this process begins at 0.001 and is decreased to 0.0001 after epoch 200. We only use the training images of KITTI 2012 for the fine-tuning process in KITTI 2012 while we merge the training images of both datasets for the fine-tuning process in KITTI 2015. The batch size is set to 4 for training on 4 NVIDIA GTX 1080Ti GPUs and the weight of six output is set as 0.5,0.5,0.5,0.7,1.0, and 1.3. The design principles of our switch training strategy will be discussed in the next section.

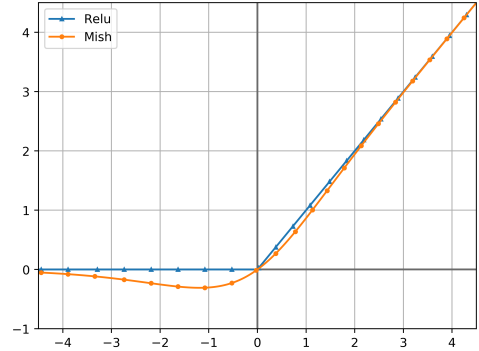


**Figure 6: Comparison between Relu and Mish**

### 4.3 Switch Training Strategy

The activation function introduces non-linearity to the neural network and plays an integral role in the network performance. Relu [11, 15, 21] and Swish [12, 24] are the two most widely used activation functions in the deep learning community. Recently, a new activation function, Mish [20] is introduced and has shown its effectiveness in many challenging missions because of its properties of unbounded above, bounded below, smooth and non-monotonic (see Figure 6 for the comparison between Relu and Mish). As shown in Table 1 we also prove Mish is a better activation function in stereo matching compared with Relu by our experiment.

Prolonging the pre-training process in SceneFlow dataset is a general method to improve the performance for the final submission to the KITTI evaluation server. But such way seems useless when we employ Mish as activation function. We think some overfitting issues may arise because of the extension of the training process and the more effective optimization and generalization capacity of Mish compared with Relu. As shown in Table 1, This is also proved by a significant decline of EPE in SceneFlow dataset but no obvious change of D1-all in KITTI 2015 dataset after the extension of the training process. Thankfully, the property of Mish makes it can directly replace activation functions like Relu without retraining a

**Table 2: Results on KITTI 2012 benchmark.**

Method	2px(%)		3px(%)		4px(%)		5px(%)		Mean Error		runtime(s)
	Noc	All	Noc	All	Noc	All	Noc	All	Noc	All	
ACFNet [34]	1.83	2.35	1.17	1.54	0.92	1.21	0.77	1.01	0.5	0.5	0.48
GANet-deep [33]	1.89	2.50	1.19	1.60	0.91	1.23	0.76	1.02	0.4	0.5	1.8
GWCNet [10]	2.16	2.71	1.32	1.70	0.99	1.27	0.80	1.03	0.5	0.5	<b>0.32</b>
SSPCVNet [28]	2.47	3.09	1.47	1.90	1.08	1.41	0.87	1.14	0.5	0.6	0.9
PSMNet [2]	2.44	3.01	1.49	1.89	1.12	1.42	0.90	1.15	0.5	0.6	0.41
GCNet [16]	2.71	3.46	1.77	2.30	1.36	1.77	1.12	1.46	0.6	0.7	0.9
MSMD-Net	<b>1.72</b>	<b>2.33</b>	<b>1.07</b>	<b>1.42</b>	<b>0.80</b>	<b>1.07</b>	<b>0.65</b>	<b>0.86</b>	<b>0.4</b>	<b>0.5</b>	0.72

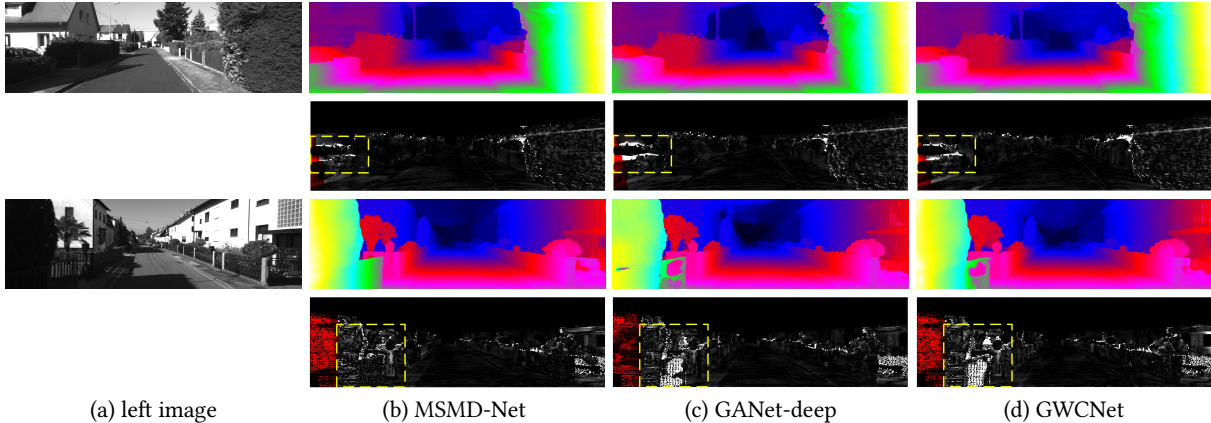


**Figure 7: Visualization results on the KITTI 2012 testset.**

new model. So we propose a switch training strategy, which first uses Relu to get a pre-trained model in SceneFlow dataset and then switch the activation function into Mish for the extension of the training process and use it to alleviate the issues discussed before. The effectiveness of our switch training strategy is proved by our experiment.

**Table 3: Ablation study results of proposed network on the Finalpass of SceneFlow dataset with our switch training strategy.**

Model	1px(%)	2px(%)	3px(%)	EPE(px)
base	8.33	4.71	3.52	0.8578
MS-Net	8.30	4.64	3.43	0.8387
MSMD-Net	<b>7.87</b>	<b>4.49</b>	<b>3.38</b>	<b>0.8197</b>

#### 4.4 Ablation Studies

In this section, we conduct ablation studies to evaluate the effectiveness of multiple scale cost volume and the refinement network. Our base model is set as removing the cost volume integration module and the refinement network. MS-Net is added the cost volume integration module while MSMD-Net preserves our whole architecture. SceneFlow and KITTI 2015 (without pretraining from Scene Flow) datasets are used to evaluate our model. As shown in Table 3 and Table 5, the multiple scale cost volume and the refinement network significantly promoted the accuracy of disparity estimation and the

best setting of MSMD-Net reached 0.8197 EPE on the SceneFlow test set and 1.86% 3-pixel error rate on the KITTI 2015 validation set.

We also conduct additional control experiments to analyze more specific model setting. In order to decrease training time, we only use KITTI 2015 dataset (without pretraining from Scene Flow) to do the control experiment. For the setting of multiple cost 3D aggregation, MS-Net is set as our control group. In the first model setting, we remove the blue lines in Figure 4, which means that we don't utilize the multi-scale cost volume. Such setting is equal to add one more stacked 3D hourglass network, so we call this new model base+. As shown in Table 5, the 3-pixel error rate improves 0.12% compared with MS-Net and is very similar to our base model, which indicates the improvement of performance is not caused by the increase of training parameters and the importance of including multiple scale cost volumes. In the second model setting, we remove one stacked 3D hourglass network to maintain a close training parameter with GWCNet. This new model is donated as MS-Net\_small. As shown in Table 5, the 3-pixel error rate improves 0.03% compared with MS-Net. Such result proves two stacked 3D hourglass network can't fully exploit the multiple scale information and it is necessary to add an additional cost volume integration module.

During the construction of warped correlation volume, the displacement is an essential hyper-parameter, which determines the disparity confidence range in the refinement network. So we also conduct a control experiment to compare the different settings of

**Table 4: Results on KITTI 2015 benchmark.**

Mehtod	All(%)			Noc(%)			Runtime(s)
	D1-bg	D1-fg	D1-all	D1-bg	D1-fg	D1-all	
CSPN [5]	1.51	<b>2.88</b>	1.74	1.40	<b>2.67</b>	1.61	1.0
GANet-deep [33]	1.48	3.46	1.81	1.34	3.11	1.63	1.8
ACFNet [34]	1.51	3.80	1.89	1.36	3.49	1.72	0.48
GWCNet [10]	1.74	3.93	2.11	1.61	3.49	1.92	<b>0.32</b>
SSPCVNet [28]	1.75	3.89	2.11	1.61	3.40	1.91	0.9
PSMNet [2]	1.86	4.62	2.32	1.71	4.31	2.14	0.41
GCNet [16]	2.21	6.16	2.87	2.02	5.58	2.61	0.9
MSMD-Net(only MS)	<b>1.42</b>	3.08	<b>1.70</b>	<b>1.31</b>	2.86	<b>1.57</b>	0.52

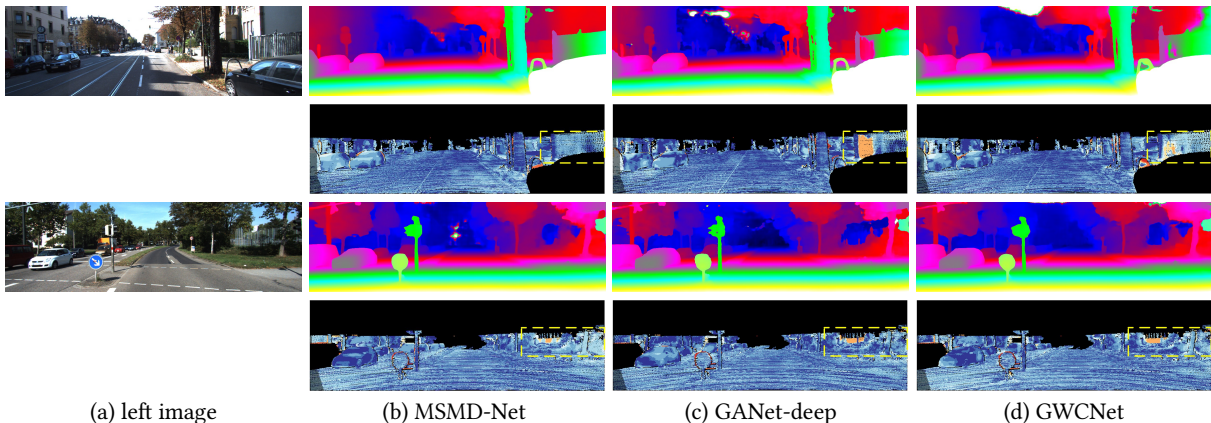


**Figure 8: Visualization results on the KITTI 2015 testset.**

**Table 5: Additional model setting comparsion on the KITTI 2015 dataset.**

Method	base	MS-Net	MSMD-Net
KITTI2015 Val Err (%)	2.08	1.94	<b>1.86</b>
Compare the setting of 3D aggregation			
Method	base+	MS-Net_small	MS-Net
KITTI2015 Val Err (%)	2.06	1.97	<b>1.94</b>
Compare of displacement setting			
Method	MSMD-Net_48	MSMD-Net_24	MSMD-Net_16
KITTI2015 Val Err (%)	1.97	<b>1.86</b>	1.90

displacement. As shown in Table 5, 24 is the best setting and a larger setting will even give a negative influence to the network.

#### 4.5 Performance on KITTI Datasets

To further evaluate our model, we compare our proposed MSMD-Net with some existing state-of-the-art methods on KITTI 2012 and KITTI 2015 datasets.

For KITTI 2012, we submit the best trained MSMD-Net to the KITTI evaluation server. As shown in Table 2, our method reached a 1.42% overall three-pixel-error rate, which surpasses GWCNet [10] and SSPCVNet [28] by 0.28% and 0.48%, respectively. The closest method is ACFNet [34] while it can't get a comparable performance in KITTI 2015, which is 0.19% lower than ours.

For KITTI 2015, we find the refinement network can't give a significant improvement to the performance. In order to reduce the computation time, the best trained MS-Net is submitted to the KITTI evaluation server. As shown in Table 4, our method reached a 1.70% overall three-pixel-error rate which surpasses GWCNet [10] and SSPCVNet [28] by 0.41%. CSPN [5] is the best published method in KITTI 2015 and we can get a better result with almost half of the computation time. Figure 7 and Figure 8 show some result examples estimated by the proposed MSMD-Net, GWCNet [10], and GANet-deep [33] in KITTI 2012 and KITTI 2015. All results are downloaded from the KITTI evaluation server and our method shows significant improvement in ill-posed regions and fence region (see dash boxes in the picture).

## 5 CONCLUSION

In this paper, we have proposed MSMD-Net to construct multi-scale and multi-dimension cost volume. The 4D multi-scale combination volume is employed to better exploit multi-scale context information and the 3D warped correlation volume is used to generate a fine-grained disparity confidence range for disparity refinement. We also introduce a switch training strategy to alleviate the over-fitting issues during training. Experimental results show the superiority of MSMD-Net on both SceneFlow and KITTI datasets. In particular, MSMD-Net ranked first on KITTI 2012 leaderboard and second on KITTI 2015 leaderboard as of June 23. Moreover, the visualization result of disparity maps demonstrates that our method



can provide better estimation on ill-posed regions (occlusion, textureless). In the future, we plan to further extend our cost volume representation to other dense matching problems such as optical flow estimation and multi-view stereo.

## REFERENCES

- [1] Joydeep Biswas and Manuela Veloso. 2011. Depth camera based localization and navigation for indoor mobile robots. In *RGB-D Workshop at RSS*, Vol. 2011. 21.
- [2] Jia-Ren Chang and Yong-Sheng Chen. 2018. Pyramid stereo matching network. In *Proceedings of the IEEE Conference on Computer Vision and Pattern Recognition*. 5410–5418.
- [3] Chenyi Chen, Ari Seff, Alain Kornhauser, and Jianxiong Xiao. 2015. Deepdriving: Learning affordance for direct perception in autonomous driving. In *Proceedings of the IEEE International Conference on Computer Vision*. 2722–2730.
- [4] Shuo Cheng, Zexiang Xu, Shilin Zhu, Zhuwen Li, Li Erran Li, Ravi Ramamoorthi, and Hao Su. 2019. Deep Stereo using Adaptive Thin Volume Representation with Uncertainty Awareness. *arXiv preprint arXiv:1911.12012* (2019).
- [5] Xinjing Cheng, Peng Wang, and Ruigang Yang. 2019. Learning Depth with Convolutional Spatial Propagation Network. *IEEE transactions on pattern analysis and machine intelligence* (2019).
- [6] Shivam Duggal, Shenlong Wang, Wei-Chiu Ma, Rui Hu, and Raquel Urtasun. 2019. DeepPruner: Learning Efficient Stereo Matching via Differentiable PatchMatch. In *Proceedings of the IEEE International Conference on Computer Vision*. 4384–4393.
- [7] Andreas Geiger, Philip Lenz, and Raquel Urtasun. 2012. Are we ready for autonomous driving? the kitti vision benchmark suite. In *2012 IEEE Conference on Computer Vision and Pattern Recognition*. IEEE, 3354–3361.
- [8] Andreas Geiger, Philip Lenz, and Raquel Urtasun. 2012. Are we ready for autonomous driving? the kitti vision benchmark suite. In *2012 IEEE Conference on Computer Vision and Pattern Recognition*. IEEE, 3354–3361.
- [9] Xiaodong Gu, Zhiwen Fan, Siyu Zhu, Zuozhuo Dai, Feitong Tan, and Ping Tan. 2019. Cascade Cost Volume for High-Resolution Multi-View Stereo and Stereo Matching. *arXiv preprint arXiv:1912.06378* (2019).
- [10] Xiaoyang Guo, Kai Yang, Wukui Yang, Xiaogang Wang, and Hongsheng Li. 2019. Group-wise correlation stereo network. In *Proceedings of the IEEE Conference on Computer Vision and Pattern Recognition*. 3273–3282.
- [11] Richard HR Hahnloser, Rahul Sarpeshkar, Misha A Mahowald, Rodney J Douglas, and H Sebastian Seung. 2000. Digital selection and analogue amplification coexist in a cortex-inspired silicon circuit. *Nature* 405, 6789 (2000), 947–951.
- [12] Soufiane Hayou, Arnaud Doucet, and Judith Rousseau. 2018. On the selection of initialization and activation function for deep neural networks. *arXiv preprint arXiv:1805.08266* (2018).
- [13] Kaiming He, Xiangyu Zhang, Shaoqing Ren, and Jian Sun. 2016. Deep residual learning for image recognition. In *Proceedings of the IEEE conference on computer vision and pattern recognition*. 770–778.
- [14] Max Jaderberg, Karen Simonyan, Andrew Zisserman, et al. 2015. Spatial transformer networks. In *Advances in neural information processing systems*. 2017–2025.
- [15] Kevin Jarrett, Koray Kavukcuoglu, Marc’Aurelio Ranzato, and Yann LeCun. 2009. What is the best multi-stage architecture for object recognition?. In *2009 IEEE 12th international conference on computer vision*. IEEE, 2146–2153.
- [16] Alex Kendall, Hayk Martirosyan, Saumitro Dasgupta, Peter Henry, Ryan Kennedy, Abraham Bachrach, and Adam Bry. 2017. End-to-end learning of geometry and context for deep stereo regression. In *Proceedings of the IEEE International Conference on Computer Vision*. 66–75.
- [17] Zhengfa Liang, Yulan Guo, Yiliu Feng, Wei Chen, Linbo Qiao, Li Zhou, Jianfeng Zhang, and Hengzhu Liu. 2019. Stereo matching using multi-level cost volume and multi-scale feature constancy. *IEEE transactions on pattern analysis and machine intelligence* (2019).
- [18] Wenjie Luo, Alexander G Schwing, and Raquel Urtasun. 2016. Efficient deep learning for stereo matching. In *Proceedings of the IEEE Conference on Computer Vision and Pattern Recognition*. 5695–5703.
- [19] Nikolaus Mayer, Eddy Ilg, Philip Hausser, Philipp Fischer, Daniel Cremers, Alexey Dosovitskiy, and Thomas Brox. 2016. A large dataset to train convolutional networks for disparity, optical flow, and scene flow estimation. In *Proceedings of the IEEE Conference on Computer Vision and Pattern Recognition*. 4040–4048.
- [20] Diganta Misra. 2019. Mish: A Self Regularized Non-Monotonic Neural Activation Function. *arXiv preprint arXiv:1908.08681* (2019).
- [21] Vinod Nair and Geoffrey E Hinton. 2010. Rectified linear units improve restricted boltzmann machines. In *Proceedings of the 27th international conference on machine learning (ICML-10)*. 807–814.
- [22] Guang-Yu Nie, Ming-Ming Cheng, Yun Liu, Zhengfa Liang, Deng-Ping Fan, Yue Liu, and Yongtian Wang. 2019. Multi-level context ultra-aggregation for stereo matching. In *Proceedings of the IEEE conference on computer vision and pattern recognition*. 3283–3291.
- [23] Jiahao Pang, Wenxiu Sun, Jimmy SJ Ren, Chengxi Yang, and Qiong Yan. 2017. Cascade residual learning: A two-stage convolutional neural network for stereo matching. In *Proceedings of the IEEE International Conference on Computer Vision Workshops*. 887–895.
- [24] Prajit Ramachandran, Barret Zoph, and Quoc V Le. 2017. Searching for activation functions. *arXiv preprint arXiv:1710.05941* (2017).
- [25] Daniel Scharstein and Richard Szeliski. 2002. A taxonomy and evaluation of dense two-frame stereo correspondence algorithms. *International journal of computer vision* 47, 1-3 (2002), 7–42.
- [26] Deqing Sun, Xiaodong Yang, Ming-Yu Liu, and Jan Kautz. 2018. Pwc-net: Cnns for optical flow using pyramid, warping, and cost volume. In *Proceedings of the IEEE Conference on Computer Vision and Pattern Recognition*. 8934–8943.
- [27] Alessio Tonioni, Fabio Tosi, Matteo Poggi, Stefano Mattoccia, and Luigi Di Stefano. 2019. Real-time self-adaptive deep stereo. In *Proceedings of the IEEE Conference on Computer Vision and Pattern Recognition*. 195–204.
- [28] Zhenyao Wu, Xinyi Wu, Xiaoping Zhang, Song Wang, and Lili Ju. 2019. Semantic Stereo Matching with Pyramid Cost Volumes. In *Proceedings of the IEEE International Conference on Computer Vision*. 7484–7493.
- [29] Gengshan Yang, Joshua Manela, Michael Happold, and Deva Ramanan. 2019. Hierarchical deep stereo matching on high-resolution images. In *Proceedings of the IEEE Conference on Computer Vision and Pattern Recognition*. 5515–5524.
- [30] Jiayu Yang, Wei Mao, Jose M Alvarez, and Miaomiao Liu. 2019. Cost Volume Pyramid Based Depth Inference for Multi-View Stereo. *arXiv preprint arXiv:1912.08329* (2019).
- [31] Fisher Yu and Vladlen Koltun. 2015. Multi-scale context aggregation by dilated convolutions. *arXiv preprint arXiv:1511.07122* (2015).
- [32] Jure Zbontar and Yann LeCun. 2015. Computing the stereo matching cost with a convolutional neural network. In *Proceedings of the IEEE conference on computer vision and pattern recognition*. 1592–1599.
- [33] Feihu Zhang, Victor Prisacariu, Ruigang Yang, and Philip HS Torr. 2019. Ga-net: Guided aggregation net for end-to-end stereo matching. In *Proceedings of the IEEE Conference on Computer Vision and Pattern Recognition*. 185–194.
- [34] Youmin Zhang, Yimin Chen, Xiao Bai, Jun Zhou, Kun Yu, Zhiwei Li, and Kuiyuan Yang. 2019. Adaptive Unimodal Cost Volume Filtering for Deep Stereo Matching. *arXiv preprint arXiv:1909.03751* (2019).